# A 15-year K-band view of long-period variables in the central region of M33

Hedieh Abdollahi*[1, 2], Mina Alizadeh[3], Fatemeh Nikzat[2], Atefeh Javadi[2], Yousefali Abedini[3,4], and Jacco Th. van Loon[5]

[1]Konkoly Observatory, HUN-REN Research Centre for Astronomy and Earth Sciences, MTA Centre of Excellence, Konkoly-Thege Miklós út 15-17, H-1121, Budapest, Hungary
[2]School of Astronomy, Institute for Research in Fundamental Sciences (IPM), P.O. Box 1956836613, Tehran, Iran
[3]Department of Physics, Faculty of Science, University of Zanjan, 38791-45371, Zanjan, Iran
[4]Center for Research in Climate Change and Global Warming (CRCC), IASBS, Zanjan, Iran
[5]Lennard-Jones Laboratories, Keele University, Keele, Staffordshire ST5 5BG, UK

**Abstract**

Long-period variables (LPVs) on the asymptotic giant branch (AGB) trace the late stages of stellar evolution and the return of mass to the interstellar medium. Their periods range from about 100 to 2000 d, so a few-year near-infrared campaign covers too few cycles for the slowest pulsators. We combine four independent UKIRT $K$-band data sets obtained between 2003 and 2018 into a homogeneous catalogue of the central ≈12 arcmin$^2$ of M33: 847 stars with 21 085 measurements over 15.11 yr. Using 82 calibration stars, we place all data on the 2MASS/Vega system and remove inter-dataset offsets of up to 0.22 mag. Of the 847 stars, 771 are variable ($\sigma_K > 0.10$ mag), and 385 have peak-to-peak amplitudes $A_K \geq 1.0$ mag, which makes them Mira candidates. Of the 156 stars with Spitzer/IRAC [3.6] photometry, 120 have $\langle K \rangle - [3.6] > 0.5$ mag and are candidate dust-enshrouded AGB stars. The catalogue is the basis for a forthcoming period–luminosity and star-formation history analysis.

***Keywords:*** *stars: AGB and post-AGB – stars: long-period variables – galaxies: individual: M33 – infrared: stars – circumstellar matter – stellar mass loss*

## 1. Introduction

During the AGB phase, low- and intermediate-mass stars can undergo large-amplitude pulsations and lose mass at rates of $10^{-8}$–$10^{-4}$ $M_\odot$ yr$^{-1}$ (Boyer et al., 2025, Gavetti et al., 2026, Höfner & Olofsson, 2018, Javadi & van Loon, 2022, Mahani et al., 2023, Mahani et al., 2026, Saremi et al., 2020, van Loon et al., 1999). As long-period variables (LPVs), they trace both a galaxy's evolved stellar population and the mass it has recently returned to the interstellar medium (e.g. Mahani et al., 2025). Near-infrared observations are particularly useful for identifying these stars in other galaxies. Dusty AGB stars that are faint at optical wavelengths can remain detectable in the K band, where their variability amplitudes are substantially larger than typical photometric errors (Whitelock et al., 2003, Wood, 1998, Wood et al., 1992).

Mira and semi-regular variables have periods of about 100–2000 d (Abdollahi et al., 2026, Goldman et al., 2019, Ita et al., 2004, Wood, 2000, Yuan et al., 2018). A 3–5 yr campaign may cover only one or two cycles of the longest-period pulsators, making it difficult to resolve period aliases or classify borderline semi-regular variables with confidence (Soszyński et al., 2004, 2009). Archival data sets can extend the baseline, but zero-point differences between instruments can then look like real variability.

M33 is well placed for this kind of study. At 955 kpc ($\mu = 24.9$ mag; Bonanos et al. 2006), its AGB stars can be resolved in the near-infrared, and its inner disc has near-solar metallicity (Bresolin, 2011, Rosolowsky & Simon, 2008). UKIRT has observed the centre of M33 since 2003, and these data were used to derive its star-formation history from the LPV population (Javadi et al., 2011a,b, 2013, 2015); the same method has since been applied to other Local Group galaxies (e.g. Abdollahi et al., 2023, 2024, Aghdam et al., 2024, Hashemi et al., 2019, Javadi et al., 2011c, Khatamsaz et al., 2026, Navabi et al., 2021, Saremi et al., 2021). Here we summarise the 15-yr $K$-band catalogue of Alizadeh et al. (2026), which combines four of these data sets, and describe the variable stars and dusty AGB candidates it contains.

*hedieh.abdollahi@csfk.org


doi: https://doi.org/10.52526/25792776-26.73.2-316

Table 1. Summary of the combined $K$-band catalogue (Alizadeh et al., 2026).

| Quantity | Value |
|---|---|
| Temporal baseline | 15.11 yr |
| Unique stars | 847 |
| $K$-band measurements | 21 085 |
| Calibration stars | 82 |
| Largest offset (UHS) | 0.22 mag |
| Variable stars ($\sigma_K > 0.10$ mag) | 771 |
| High-amplitude stars ($A_K \geq 1.0$ mag) | 385 |
| Stars with Spitzer [3.6] | 156 |
| Dusty candidates ($\langle K \rangle - [3.6] > 0.5$ mag) | 120 |

## 2. Data and catalogue construction

The first data set is the UIST (Ramsay Howat et al., 2004) monitoring programme of 2003–2007: 50 exposures over 23 nights, a median of 12 epochs per star and a baseline of 3.80 yr. It contains 18 398 sources with a typical precision of 0.02 mag for $K < 17$ mag (Javadi et al., 2011a). The second is a UFTI (Roche et al., 2003) mosaic from August 2005, co-added from 30 frames, for which PSF photometry is presented here for the first time. The third is WFCAM (Casali et al., 2007) imaging from 2005–2007, for which we made new PSF photometry of the four central tiles (Alizadeh et al., 2025b). The fourth is a single epoch from November 2018 taken from the UKIRT Hemisphere Survey (UHS) DR3 (Schneider et al., 2025).

The UIST, UFTI and WFCAM images were reduced with DAOPHOT/ALLSTAR (Nikzat et al., 2013, Stetson, 1987); for WFCAM, an empirical PSF was built from isolated bright stars in each frame. The UHS epoch was reduced with PHOTUTILS v1.13 (Bradley et al., 2024), part of the Astropy ecosystem (Astropy Collaboration et al., 2022). A comparison on an archival UFTI H-band frame reduced with both codes gave a mean difference of +0.036 mag (PHOTUTILS − DAOPHOT) for 1522 common sources, with a standard deviation of 0.074 mag and a median absolute deviation of 0.048 mag. All photometry in the catalogue is PSF-based. The central field is very crowded: In the UHS source catalogue, about 62 per cent of detected sources within 1 arcmin of the nucleus belong to blended groups, and aperture photometry in this region is biased by the light of close neighbours (Alizadeh et al., 2024, 2025a, 2026). This is why the earlier aperture-based WFCAM catalogue (Javadi et al., 2015) is not used.

All catalogues were matched to the UIST astrometric frame with a 0.5 arcsec radius; the median separation is 0.14 arcsec. We kept stars detected in at least two data sets. The final catalogue has 847 stars and 21 085 $K$-band measurements over 15.11 yr (2003 October to 2018 November), and covers $\approx$12 arcmin$^2$ ($\approx$0.9 kpc$^2$). Each star has between 4 and 63 epochs, with a median of 21. The main properties are listed in Table 1.

## 3. Photometric homogenisation

Each data set was reduced independently, so each has its own zero point. Left uncorrected, these offsets would appear as long-term brightness changes. We adopted UFTI as the reference, since it is calibrated to 2MASS/Vega (Skrutskie et al., 2006) as in earlier papers of the series. As calibration stars, we selected those detected in all four data sets, with $K < 17$ mag and an rms scatter below 0.20 mag. This gives 82 stars with $K = 13.9$–$17.0$ mag.

For each of the other data sets, we applied a constant correction equal to the median magnitude difference from UFTI over these 82 stars (uncertainty $\approx$0.015 mag). We define the offset as $\Delta K = K_{\rm dataset} - K_{\rm UFTI}$. The measured median offsets are +0.005 mag for UIST, -0.096 mag for WFCAM and +0.218 mag for UHS; we applied corrections of the opposite sign to bring each data set onto the UFTI reference scale. The large UHS value mostly reflects the arbitrary zero point of the PHOTUTILS reduction. None of the offsets depends significantly on magnitude.

After the correction, the scatter decreased for 58 of the 82 calibration stars (71 per cent). The mean change was −11.8 per cent and the median −15.2 per cent. The remaining 24 stars are not strictly constant (rms 0.07–0.19 mag), and for such stars a constant shift can either raise or lower the scatter, depending on which pulsation phases were observed.


doi: https://doi.org/10.52526/25792776-26.73.2-316

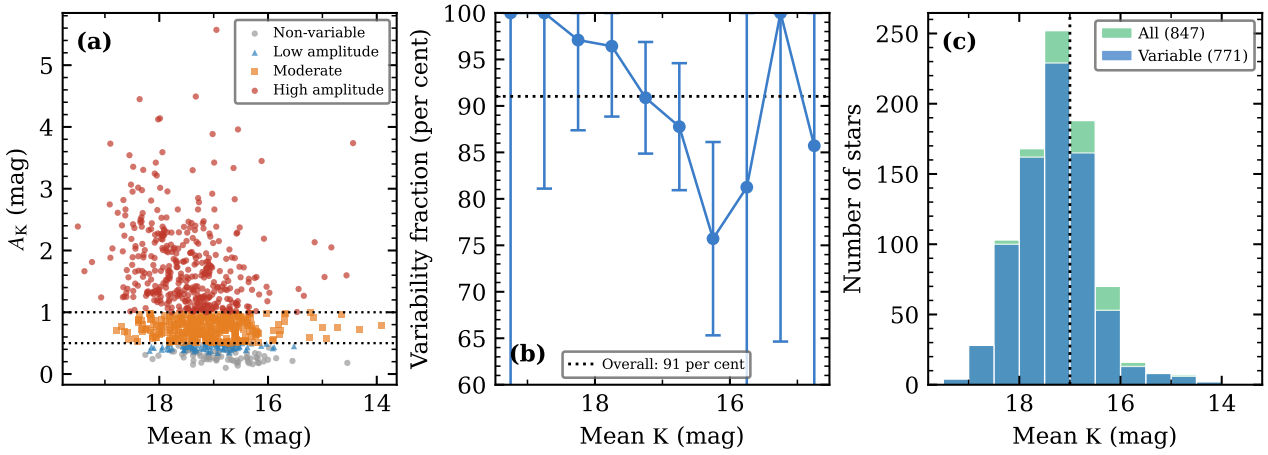


Figure 1. Variability statistics as a function of mean $K$ magnitude for the 847 stars. (a) Peak-to-peak amplitude $A_K$, colour-coded by class; the dotted lines mark the class boundaries at 0.5 and 1.0 mag. (b) Fraction of variable stars in 0.5-mag bins, with $1\sigma$ Poisson errors; the dotted line marks the overall 91 per cent. (c) $K$-band luminosity function of all stars (green) and of the 771 variables (blue); the dotted line marks $K = 17$ mag. Adapted from Alizadeh et al. (2026).

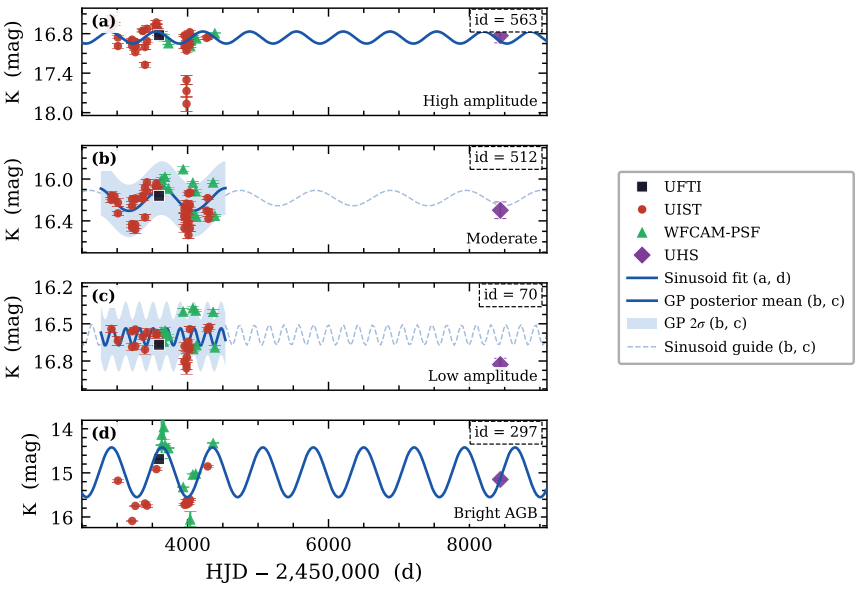


Figure 2. Example $K$-band light curves combining all four data sets ($1\sigma$ errors; the UHS 2018 point is on the right): (a) star 563 ($A_K = 2.39$ mag), (b) star 512 ($A_K = 0.63$ mag), (c) star 70 ($A_K = 0.49$ mag), and (d) the bright AGB star 297 ($A_K = 2.13$ mag, $\langle K \rangle = 14.81$ mag). Curves only guide the eye: a Gaussian-process mean with a $2\sigma$ band in (b) and (c), and a sinusoid at the Lomb–Scargle period in (a) and (d). Figure from Alizadeh et al. (2026).

## 4. The variable population

For each star we computed the scatter of the homogenised magnitudes,

$$\sigma_K = \left[ \frac{1}{N-1} \sum_{i=1}^{N} \left( K_i - \bar{K} \right)^2 \right]^{1/2}, \tag{1}$$

where $N$ is the number of measurements and $\bar{K}$ is the unweighted mean magnitude. A star is classed as variable if $\sigma_K > 0.10$ mag, about five times the typical precision. This applies to 771 of the 847 stars (91 per cent). The fraction is high because the catalogue contains bright stars detected in several surveys, which are mostly AGB stars; it does not describe the whole stellar population of M33.

As a measure of amplitude, we use the peak-to-peak range $A_K = K_{\max} - K_{\min}$, which does not depend on a period. For the 17 stars with ten or fewer epochs, it is a lower limit. A further 21 stars pass the variability threshold because of a single deviant epoch; they are kept but flagged. We divide the variables into three amplitude classes (Fig. 1a): 385 high-amplitude stars ($A_K \geq 1.0$ mag, mean $A_K = 1.77$ mag), 308 moderate-amplitude stars ($0.5 \leq A_K < 1.0$ mag) and 78 low-amplitude stars ($A_K < 0.5$ mag). The other 76 stars are not variable. These classes are descriptive and may change once periods are determined. Example light curves are shown in Fig. 2.


doi: https://doi.org/10.52526/25792776-26.73.2-316

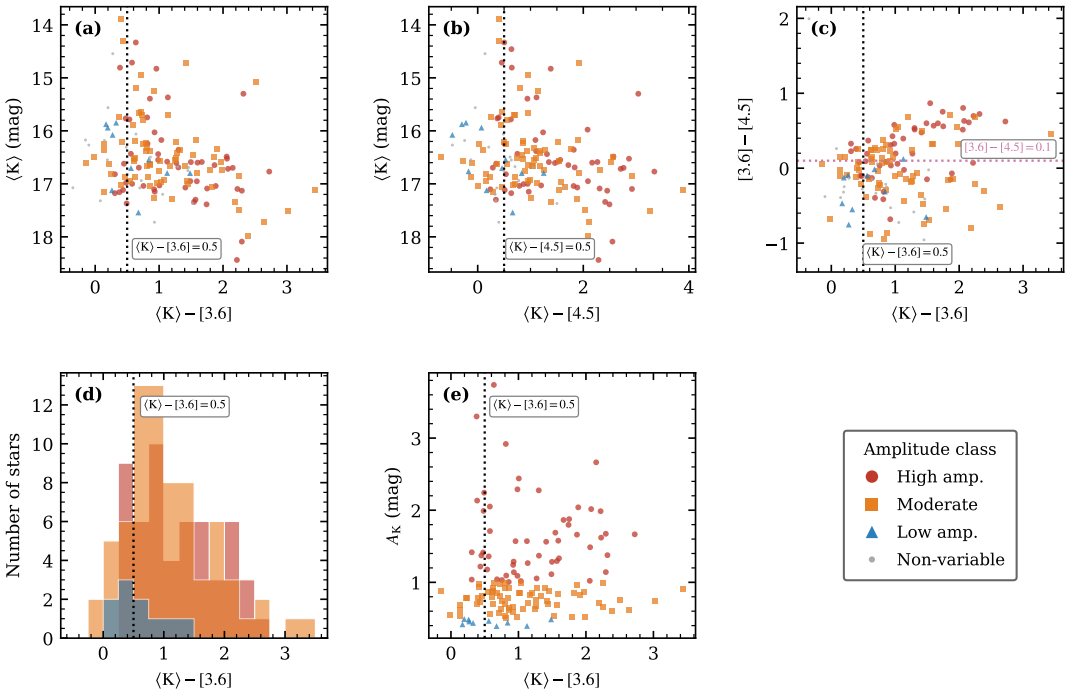


Figure 3. Near- to mid-infrared colours of the Spitzer-matched stars, colour-coded by amplitude class: (a) $\langle K\rangle$ vs. $\langle K\rangle - [3.6]$; (b) $\langle K\rangle$ vs. $\langle K\rangle - [4.5]$; (c) $[3.6] - [4.5]$ vs. $\langle K\rangle - [3.6]$; (d) $\langle K\rangle - [3.6]$ distribution per class; (e) $A_K$ vs. $\langle K\rangle - [3.6]$. Purple line in (c): DUSTiNGS extreme-AGB limit, $[3.6] - [4.5] = 0.1$ mag (Boyer et al., 2015). Black dotted line: our dusty-candidate threshold, $\langle K\rangle - [3.6] = 0.5$ mag. Figure from Alizadeh et al. (2026).

The variable fraction lies between 76 and 100 per cent at all magnitudes (Fig. 1b). The luminosity function (Fig. 1c) peaks near $K \approx 17$ mag, or $M_K \approx -7.9$ mag at $\mu = 24.9$ mag, close to the tip of the thermally pulsing AGB. The catalogue becomes incomplete fainter than $K \approx 18$ mag.

## 5. Dusty AGB candidates

Circumstellar dust absorbs stellar radiation and re-emits it at infrared wavelengths, making the $\langle K\rangle - [3.6]$ colour a useful indicator of circumstellar dust emission (McQuinn et al., 2007, SSC & IRSA, 2020). We accepted a match only when the two sources were each other's nearest neighbours within 1 arcsec. In total, 156 stars have valid [3.6] photometry (114 from SEIP and 42 from McQuinn et al. (2007)).

Of these, 120 have $\langle K\rangle - [3.6] > 0.5$ mag and are candidate dust-enshrouded AGB stars (Fig. 3). This number is a lower limit. Only 18 per cent of the catalogue has a Spitzer counterpart. This low fraction is largely attributable to crowding in the nuclear field and should not be interpreted as evidence that the remaining stars lack circumstellar dust. Such stars are hard to reach in the optical: even the brightest star in our sample ($\langle K\rangle = 13.88$ mag) would have $V > 18.9$ mag for $V - K = 5$ mag, below the $V < 17$ mag limit of ASAS-SN (Jayasinghe et al., 2018).

## 6. Discussion and conclusions

The main gain is the length of the baseline. For a Mira with $P = 500$ d, UIST alone covers about 2.8 cycles, while the full 15.11-yr series covers about 11. For $P \sim 1500$ d, the combined data cover about 3.7 cycles, whereas UIST alone does not complete one. The 11-year gap between the final WFCAM epoch and the UHS observation extends the baseline and provides a late-time measurement that may help identify long-term changes in stellar brightness.

In summary, the four UKIRT data sets, placed on one photometric system, give a 15-yr $K$-band time series for the central region of M33 (Table 1). Most stars in it are variable AGB stars; 385 of them are Mira candidates, and at least 120 are candidate dust-enshrouded AGB stars that can be difficult to identify


doi: https://doi.org/10.52526/25792776-26.73.2-316

in optical surveys. Our next step is to determine periods and derive period–luminosity relations, mass-loss rates, and the star-formation history from this sample.

## References


Abdollahi H., 2026, TRGB Distances to the Andromeda Dwarf Satellites from the INT Monitoring Survey (arXiv:2611.08648), https://arxiv.org/abs/2611.08648

Abdollahi H., et al., 2023, ApJ, 948, 63

Abdollahi H., Javadi A., van Loon J. T., McDonald I., Abdollahi M., Saremi E., Khosroshahi H. G., Mahani H., 2024, Communications of the Byurakan Astrophysical Observatory, 71, 383

Abdollahi H., et al., 2026, ApJ, 1000, 69

Aghdam S. T., et al., 2024, Astrophys. J. , 972, 47

Alizadeh M., Javadi A., van Loon J. T., Abedini Y., Abdollahi H., Seifipour S., 2024, Communications of the Byurakan Astrophysical Observatory, 71, 389

Alizadeh M., Abedini Y., Abdollahi H., 2025a, Unveiling Long-Period Variables in M33's Central Region: Insights into Stellar Evolution and Star Formation via Near-Infrared Photometry (arXiv:2512.18423), https://arxiv.org/abs/2512.18423

Alizadeh M., Abedini Y., Abdollahi H., 2025b, Communications of the Byurakan Astrophysical Observatory, 72, 294

Alizadeh M., Javadi A., Abedini Y., Nikzat F., Abdollahi H., van Loon J. T., 2026, Monthly Notices of the Royal Astronomical Society

Astropy Collaboration et al., 2022, ApJ, 935, 167

Bonanos A. Z., et al., 2006, ApJ, 652, 313

Boyer M. L., et al., 2015, ApJS, 216, 10

Boyer M. L., et al., 2025, Astrophys. J. , 991, 24

Bradley L., et al., 2024, astropy/photutils: 1.13.0, Zenodo, doi:10.5281/zenodo.12585239

Bresolin F., 2011, ApJ, 730, 129

Casali M., et al., 2007, A&A, 467, 777

Gavetti C., et al., 2026, Astrophys. J. , 1006, 131

Goldman S. R., et al., 2019, ApJ, 877, 49

Hashemi S. A., Javadi A., van Loon J. T., 2019, Mon. Not. R. Astron. Soc. , 483, 4751

Höfner S., Olofsson H., 2018, A&ARv, 26, 1

Ita Y., et al., 2004, MNRAS, 347, 720

Javadi A., van Loon J. T., 2022, in Decin L., Zijlstra A., Gielen C., eds, IAU Symposium Vol. 366, The Origin of Outflows in Evolved Stars. pp 210–215 (arXiv:2204.08944), doi:10.1017/S1743921322001326

Javadi A., van Loon J. T., Mirtorabi M. T., 2011a, MNRAS, 411, 263

Javadi A., van Loon J. T., Mirtorabi M. T., 2011b, MNRAS, 414, 3394

Javadi A., van Loon J. T., Mirtorabi M. T., 2011c, in Kerschbaum F., Lebzelter T., Wing R. F., eds, Astronomical Society of the Pacific Conference Series Vol. 445, Why Galaxies Care about AGB Stars II: Shining Examples and Common Inhabitants. ASP, p. 497 (arXiv:1101.5271), doi:10.48550/arXiv.1101.5271

Javadi A., van Loon J. T., Khosroshahi H., Mirtorabi M. T., 2013, MNRAS, 432, 2824

Javadi A., Saberi M., van Loon J. T., Khosroshahi H., Golabatooni N., Mirtorabi M. T., 2015, MNRAS, 447, 3973

Jayasinghe T., et al., 2018, MNRAS, 477, 3145

Khatamsaz F., Abdollahi M., Javadi A., Mahani H., van Loon J. T., Abdollahi H., Ghaziasgar S., 2026, A Study on the Evolution of NGC6822. I. Investigating the Star Formation History through Evolved Stellar Populations (arXiv:2609.34329), https://arxiv.org/abs/2609.34329

Mahani H., et al., 2023, in Wong T., Kim W.-T., eds, IAU Symposium Vol. 373, Resolving the Rise and Fall of Star Formation in Galaxies. pp 264–267, doi:10.1017/S1743921322004951

Mahani H., et al., 2025, ApJ, 992, 94

Mahani H., Rostami N., Javadi A., Abdollahi H., van Loon J. T., Kemper F., Sanchez-Monge A., 2026, SEDust: A DUSTY-Based SED-Fitting Pipeline for Dust and Mass-Loss from AGB and LPV Stars (arXiv:2611.09086), https://arxiv.org/abs/2611.09086

McQuinn K. B. W., et al., 2007, ApJ, 664, 850

Navabi M., et al., 2021, Astrophys. J. , 910, 127

Nikzat F., Javadi A., Mirtorabi M. T., van Loon J. T., Khosroshahi H., 2013, IAU Symposium, 292, 160

Ramsay Howat S. K., et al., 2004, in Moorwood A. F. M., Iye M., eds, Proc. SPIE Vol. 5492, Ground-based Instrumentation for Astronomy. SPIE, Bellingham, p. 1160, doi:10.1117/12.551673

Roche P. F., et al., 2003, in Iye M., Moorwood A. F. M., eds, Proc. SPIE Vol. 4841, Instrument Design and Performance for Optical/Infrared Ground-based Telescopes. SPIE, Bellingham, p. 901, doi:10.1117/12.460987

Rosolowsky E., Simon J. D., 2008, ApJ, 675, 1213

SSC IRSA 2020, Spitzer Enhanced Imaging Products (SEIP), IPAC, doi:10.26131/IRSA433

Saremi E., et al., 2020, Astrophys. J. , 894, 135

Saremi E., Javadi A., Navabi M., van Loon J. T., Khosroshahi H. G., Bojnordi Arbab B., McDonald I., 2021, Astrophys. J. , 923, 164

Schneider A. C., et al., 2025, AJ, 170, 86

Skrutskie M. F., et al., 2006, AJ, 131, 1163

Soszyński I., Udalski A., Kubiak M., Szymański M., Pietrzyński G., Żebruń K., Szewczyk O., Wyrzykowski Ł., 2004, Acta Astronomica, 54, 129

Soszyński I., et al., 2009, Acta Astronomica, 59, 239

Stetson P. B., 1987, PASP, 99, 191

Whitelock P. A., Feast M. W., van Loon J. T., Zijlstra A. A., 2003, MNRAS, 342, 86

Wood P. R., 1998, A&A, 338, 592

Wood P. R., 2000, PASA, 17, 18

Wood P. R., Whiteoak J. B., Hughes S. M. G., Bessell M. S., Gardner F. F., Hyland A. R., 1992, ApJ, 397, 552

Yuan W., Macri L. M., Javadi A., Lin Z., Huang J. Z., 2018, Astron. J. , 156, 112

van Loon J. T., Groenewegen M. A. T., de Koter A., Trams N. R., Waters L. B. F. M., Zijlstra A. A., Whitelock P. A., Loup C., 1999, A&A, 351, 559